European Journal of Medicinal Chemistry 122 (2016) 185–195

Contents lists available at ScienceDirect

European Journal of Medicinal Chemistry

journal homepage: http://www.elsevier.com/locate/ejmech

Research paper

Novel (2,6-difluorophenyl)(2-(phenylamino)pyrimidin-4-yl) methanones with restricted conformation as potent non-nucleoside reverse transcriptase inhibitors against HIV-1

Petr Šimon [a], Ondřej Baszczyňski [a], David Šaman [a], George Stepan [b], Eric Hu [b], Eric B. Lansdon [b], Petr Jansa [b], Zlatko Janeba [a, *]

[a] Institute of Organic Chemistry and Biochemistry, Czech Academy of Sciences, Flemingovo nám. 2, Prague-6 CZ-16610, Czech Republic
[b] Gilead Sciences Inc., 333 Lakeside Drive, Foster City, CA 94404, USA

ARTICLE INFO

Article history:
Received 15 April 2016
Received in revised form
1 June 2016
Accepted 15 June 2016
Available online 17 June 2016

Keywords:
Diarylpyrimidine (DAPY)
Etravirine
Human immunodeficiency virus (HIV)
Non-nucleoside reverse transcriptase inhibitors
NNRTIs
Rilpivirine

ABSTRACT

To elucidate the structure-geometry-activity relationship in diarylpyrimidine family (DAPYs) containing carbonyl linker between the central pyrimidine core and phenyl type B-arm, a series of (2,6-difluorophenyl)(2-(phenylamino)pyrimidin-4-yl)methanones was designed, prepared and tested for their anti-HIV-1 activity. The carbonyl linker bearing B phenyl arm was successfully attached at both C-2 and C-4 positions of the central pyrimidine ring using a new synthetic approach. Further modifications of target compounds are present at C-5 position of the pyrimidine ring. *In vitro* anti-HIV-1 activity study performed on a series of 22 compounds confirmed the crucial importance of both conformational rigidity between phenyl B arm and the pyrimidine core linked through the carbonyl bridge, as well as presence of fluoro substituents in *ortho*-positions of phenyl B moiety. The most potent derivative of the series, compound **17**, having almost perpendicular angle within the two planes made from the B aromatic arm and the pyrimidine ring, exhibited low nanomolar anti-HIV-1 activity (EC_{50} = 4 nM) with no significant toxicity (CC_{50} > 57.1 μM).

1. Introduction

Etravirine (Fig. 1) [1–3] and rilpivirine (Fig. 1) [4,5] represent highly potent and FDA approved non-nucleoside reverse transcriptase inhibitors (NNRTIs) of human immunodeficiency virus (HIV-1) [6–11]. NNRTIs play an important role in highly active antiretroviral therapy (HAART) and in prevention and treatment of HIV infections. Due to the emergence of severe side effects and due to the development of multidrug-resistant HIV strains, intensive and continuous efforts have led to the identification of a number of promising NNRTIs hits, leads, and candidates [12–17]. Etravirine and rilpivirine belong to the diarylpyrimidine (DAPY) family and specifically bind to an allosteric hydrophobic site of reverse transcriptase (RT) of HIV [6]. As RT function is utterly essential in the HIV lifecycle, the area of DAPY analogues has been intensively studied during the last two decades due to their high potency [6–17]. Especially, determination of crystal structures of HIV-1 RT with the approved NNRTIs had key implications for further drug design [18].

A large number of SAR studies on DAPY analogues were performed covering various substitutions of the aromatic rings, as well as diverse linkers between C-4 position of the pyrimidine ring and aryl moiety B (Fig. 2a). Among the latter modifications, carbon based linkers have been extensively studied, namely compounds having linkers such as: a) carbonyl group [19] or its derivatives as Schiff bases with hydrazine [20] or hydroxylamine [21] (such analogues were low nanomolar inhibitors of HIV-1 RT); b) (cyclopropylamino)methylenes [22] and (alkylamino)methylenes [23] (prepared by reduction of the corresponding imino derivatives); c) hydroxymethylene moiety (prepared by reduction of the carbonyl linker) [24]; d) halomethylene [25] and cyanomethylene [26] linkers (with comparable potency to analogues with the hydroxymethylene linkers); e) hydroxyl(alkyl)methylene linkers [27] (formed by the reaction of the corresponding alkylmagnesium reagent with the carbonyl group); and f) $-CH_2$-NH- diatomic linker [28] (to improve conformational flexibility and positional adaptability of traditional DAPY compounds).

* Corresponding author.
E-mail address: janeba@uochb.cas.cz (Z. Janeba).

http://dx.doi.org/10.1016/j.ejmech.2016.06.026
0223-5234/

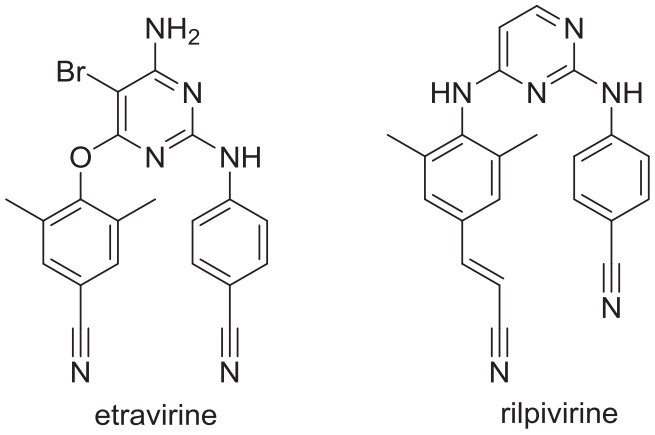

Fig. 1. Structures of the FDA approved NNRTIs – etravirine and rilpivirine.

When comparing anti-HIV-1 activity of previously published compounds with methylene or carbonyl linker (Fig. 2a) their activity strongly depends on the position of substituents on B aryl ring. Presence of substituents in both C-2 and C-6 positions of phenyl B ring is crucial for the biological activity of NNRTIs, as is also the case of 2,6-dimethylphenyl moiety in etravirine and rilpivirine (Fig. 1). The two *ortho*-substituents generate almost perpendicular geometry of B aryl ring towards the pyrimidine plane and modulation at both B ring *ortho*-positions resulted in a significant increase of anti-HIV-1 activity [29]. Such structural features were previously combined in compounds bearing B aryl ring substituted with either chloro [30], bromo [30], and fluoro [31] atoms in both *ortho*-positions. In particular, the recently reported series based on a combination of structural features of DAPY and DABO (dihydroxy-alkoxy-benzyl-oxopyrimidines) analogues and bearing 2,6-difluorophenyl B ring (Fig. 2b) exhibited nanomolar anti-HIV-1 activity against wild-type, as well as clinically relevant mutant strains [31]. Based on the above data we have designed and synthesized a novel series of NNRTIs having 2,6-difluorobenzoyl moiety (as B arm) at C-4 position of the central pyrimidine core (Fig. 2c).

2. Results and discussion

2.1. Chemistry

The reported synthetic pathways leading to carbonyl modified DAPY derivatives usually consist of two key synthetic sequences [19]: 1) the (4-cyanophenyl)amino moiety is connected to C-2 position of the pyrimidine ring; 2) the chlorine atom in C-4 position of pyrimidine is replaced by a second aromatic arm, using correspondingly substituted phenylacetonitriles under basic conditions. But, such a synthetic approach has not been successful to produce the desired analogues bearing 2,6-difluorophenyl B arm connected to the central pyrimidine core *via* the carbonyl linker. To overcome this synthetic obstacle, we have designed new synthetic sequence where B arm is attached to 2,4-dichloropyrimidine in the first step, followed by the subsequent modification of C-2 position of the pyrimidine ring [32]. In order to test the efficiency of such synthetic approach and to easily characterize the two possible regioisomers formed in the first reaction step, namely in the reaction of 2,4-dichloropyrimidine with the corresponding arylaldehyde, several model compounds without *ortho*-substituents on B phenyl ring were synthesized first (Scheme 1).

Thus, commercially available 2,4-dichloropyrimidine was reacted with 4-formylbenzonitrile under the *N*,*N*-dimethylbenzimidazolium iodide catalysis [33] to give a mixture of regioisomers **1** and **2** (Scheme 1) in a 4:3 ratio (20% and 15% yields, respectively). Analogous reaction of 4-methoxybenzaldehyde with 2,4-dichloropyrimidine afforded only the desired regioisomer **3** (Scheme 1), modified at C-4 position of pyrimidine, though in low 27% yield. Intermediates **1**–**3** were subsequently treated with 4-aminobenzonitrile under the Buchwald coupling conditions [34] to yield corresponding derivatives **4**–**6** (Scheme 1) in satisfactory yields (53–68%). Although the synthesis of compounds **4** [22] and **6** [19] has recently been reported, the original synthetic route consisted of five steps offering the final products in significantly lower

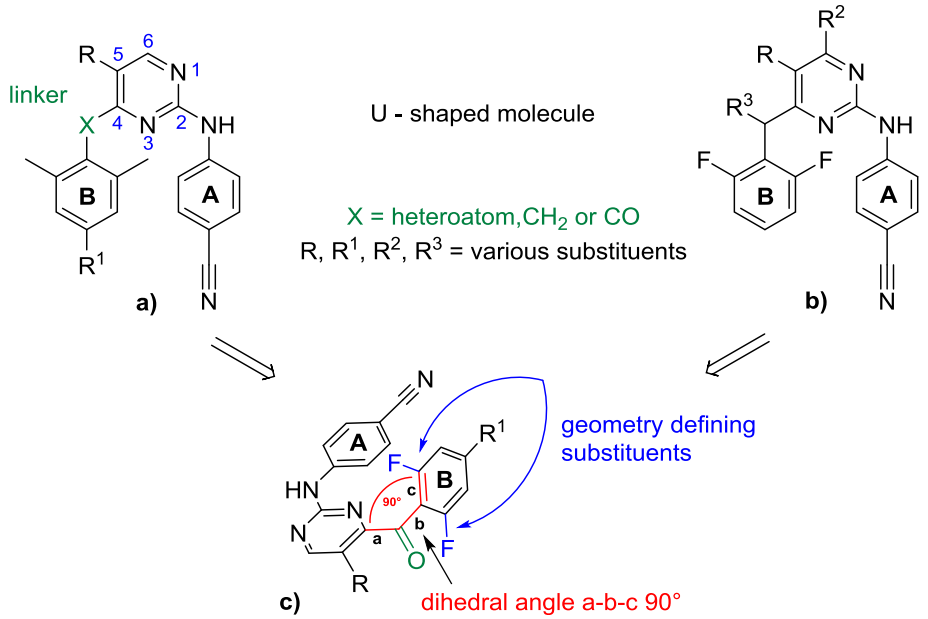

Fig. 2. a) Numbering and general structure of DAPY analogues; b) structure of potent DAPY–DABO hybrides [31]; c) geometry and structure of target molecules featuring the carbonyl linker and 2,6-difluorophenyl B ring.

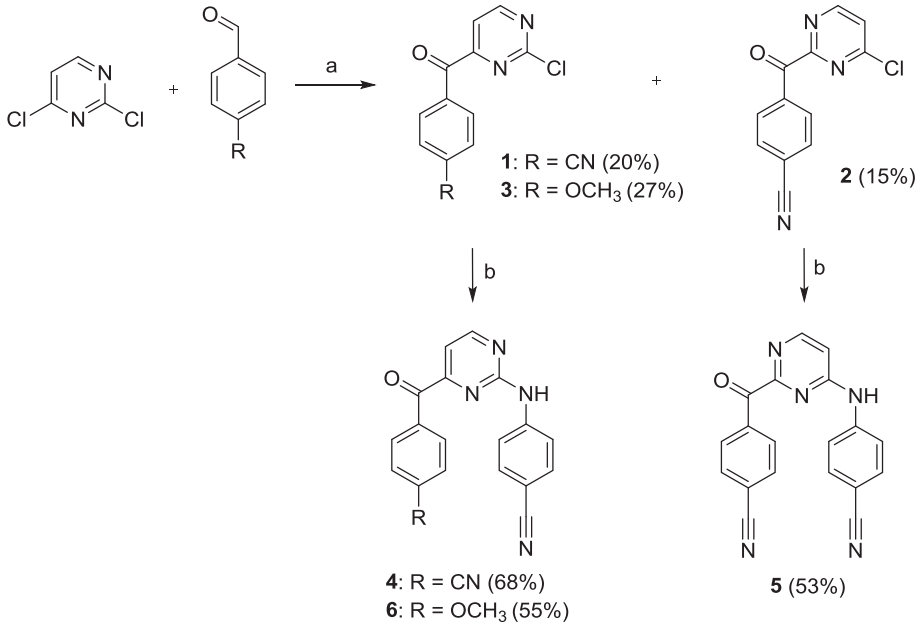

Scheme 1. Reagents and conditions: (a) NaH, *N*,*N*-dimethylbenzimidazolium iodide, DMF, r.t., 4 h; (b) 4-aminobenzonitrile, $Pd(OAc)_2$, XantPhos, Cs_2CO_3, dioxane, 100 °C, 4 h.

overall yields compared to our novel approach.

For correct assignment of true structures of pyrimidine regioisomers **1** and **2** (Scheme 1), and subsequently of the whole NNRTIs series (see details in 2.2 chapter of NMR studies), the hydroxymethylene derivatives **7** and **8** (Scheme 2) were prepared from compounds **4** and **5**, respectively, using sodium borohydride in MeOH [24].

In order to prepare structural analogues of etravirine (Fig. 1), compounds **4**–**6** were converted into their 5-bromopyrimidine derivatives **9**–**11** (Scheme 2) using *N*-bromosuccinimide (NBS). The yields of the bromination highly depend on the aryl substitution of B phenyl arm as quite complex mixtures were observed in the cases of electron withdrawing 4-cyano group. In this case, desired 5-bromopyrimidines **9** (17%) and **11** (3%), as well as the by-product **12** (8%, Scheme 2), were obtained in very low yields. Electron richer derivative **10** (Scheme 2) was, on the other hand, isolated in a 92% yield.

Subsequently, the intended NNRTIs series bearing 2,6-difluorobenzoyl moiety as B arm was prepared using the above developed reaction sequence. First, the reactions of 2,4-dichloropyrimidine with 4-substituted 2,6-difluorobenzaldehydes under the *N*,*N*-dimethylbenzimidazolium iodide catalysis [33] yielded intermediates **13**–**15** (Scheme 3) in variable yields (28–73%). Bromo derivative **15** was then converted into cyano analogue **16** (Scheme 3) in 88% yield using Negishi coupling conditions. The reaction of 2-chloropyrinidine derivatives **13**, **14** and **16** with 4-aminobenzonitrile under Buchwald coupling conditions [34] afforded the desired products **17**–**19** (Scheme 3) in moderate yields. When the Buchwald reaction was applied to bromo derivative **15**, both halogen atoms were replaced with 4-aminobenzonitrile giving derivative **20** (Scheme 3) in 18% yield.

Finally, bromination of derivative **17** using NBS in DMF afforded both desired 5-bromopyrimidine derivative **21** (12%) and bis-brominated by-product **22** (13%, Scheme 4). To evaluate the

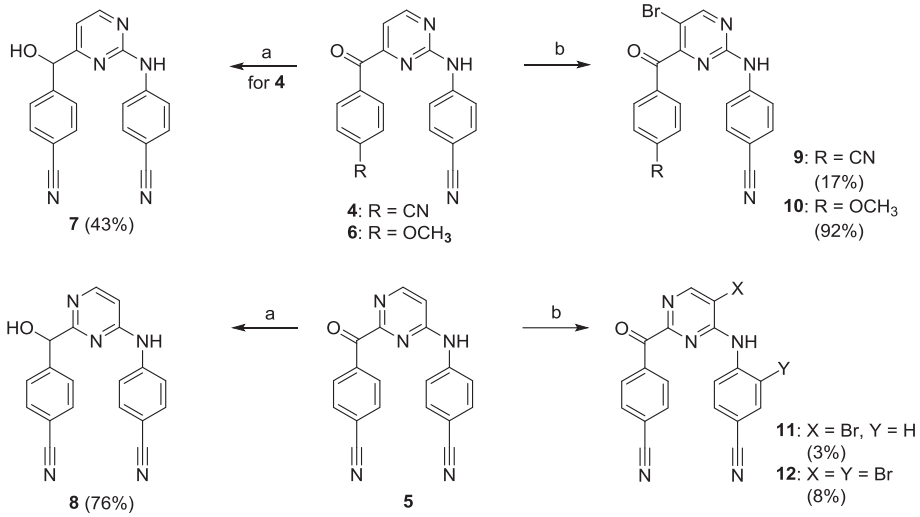

Scheme 2. Reagents and conditions: (a) $NaBH_4$, MeOH, r.t., 1 h; (b) NBS, DMF, 100 °C, overnight.

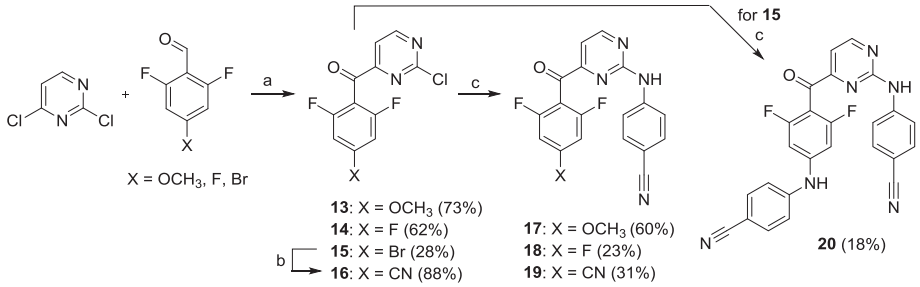

Scheme 3. Reagents and conditions: (a) NaH, *N*,*N*-dimethylbenzimidazolium iodide, dioxane, 80 °C, overnight; (b) $Zn(CN)_2$, $Pd(t\text{-}Bu_3P)_2$, DMF, 80 °C, 1 h; (c) 4-aminobenzonitrile, $Pd(OAc)_2$, XantPhos, Cs_2CO_3, dioxane, 100 °C, 4 h.

biological effect of the 4-methoxy versus 4-hydroxy group present on B phenyl ring, compound **21** was treated with boron tribromide in DMC to give derivative **23** (in 9% yield, Scheme 4).

2.2. NMR studies

The pyrimidine regioisomers modified either in C-2 or in C-4 positions have very similar ^1H and ^{13}C NMR spectra. Due to lack of protons in such derivatives the unambiguous assignment of carbon signals and confirmation of the structures are difficult. Generally, the 2D NMR HSQC and HMBC spectra are used. Unfortunately, it is quite a complicated task to distinguish between positions of the substituents in isomeric compounds **1** and **2**, as well as **4** and **5** (Scheme 1) due to the absence of cross peaks Py-H5/C=O. In order to determine the absolute structures we decided to reduce the carbonyl function in compounds **4** and **5** to prepare the corresponding hydroxymethyl analogues **7** and **8** (Scheme 2). The ability to observe CH–OH/Py-C5 interaction allowed us to unequivocally confirm the structure of compound **7**.

2.3. Biological activity

The prepared carbonyl bridged DAPY analogues were tested for their *in vitro* anti-HIV-1 activity (Table 1). Compounds **17**–**21** exhibited submicromolar activities and no or low cytotoxicity. The common structural feature of the most potent compounds is 4-cyanophenyl as A ring and 4-substituted 2,6-difluorobenzoyl as B arm. The most active compound **17** (EC_{50} = 4 nM) represents new NNRTIs lead structure for further optimization.

Evidently, the synthetic intermediates, namely compounds **1**–**3** and **13**–**16**, lacking the 4-aminobenzonitrile moiety (A arm) do not possesses any antiviral properties (Table 1). This corroborates the relevance of U-shaped diarylpyrimidine structural feature for potent antiretroviral properties of DAPY analogues. Furthermore, the absence of one or two *ortho*-substituents on B ring in DAPY series (compounds **11** and **4**–**10**, respectively) does not lead to substantial perpendicular geometry of B aryl moiety towards the central pyrimidine plane, which explains much worse (several orders of magnitude) anti-HIV-1 activity of these compounds (Table 1).

Finally, as the effectiveness of current NNRTI agents is usually hampered by the rapid emergence of drug-resistant viruses, there is an urgent need to develop novel NNRTIs without such a

Table 1
Anti-HIV activity and toxicity of all tested derivatives (n = 2).

Compound	EC_{50}-MT4 (μM)	CC_{50}-MT4 (μM)	SI[a]
1	>57	31.9	<0.56
2	>57	16.5	<0.29
3	>57	39.6	<0.69
4[b]	4.5	>57	>12.7
5	43	>57	>1.33
6[c]	0.814	>57	>70.0
7	3.7	>57	>15.4
8	>57	>57	~1.00
9	7.4	>57	>7.70
10	>57	2.45	<0.04
11	27.7	>57	>2.06
13	>57	>57	~1.00
14	>57	40.1	<0.70
15	>57	>57	~1.00
16	>57	30.5	<0.54
17	0.004	>57	>14,250
18	0.034	>57	>1676
19	0.051	>57	>1118
20	0.310	51.9	167
21	0.069	38.7	561
22	18.9	>57	>3.02
23	>57	>57	~1.00
Etravirine	0.002	5.88	2940
Efavirenz	0.001	20.6	20,600

[a] Selectivity index: CC_{50}/EC_{50} ratio.
[b] Known compound **4** [22].
[c] Known compound **6** with reported EC_{50} = 0.239 μM [19].

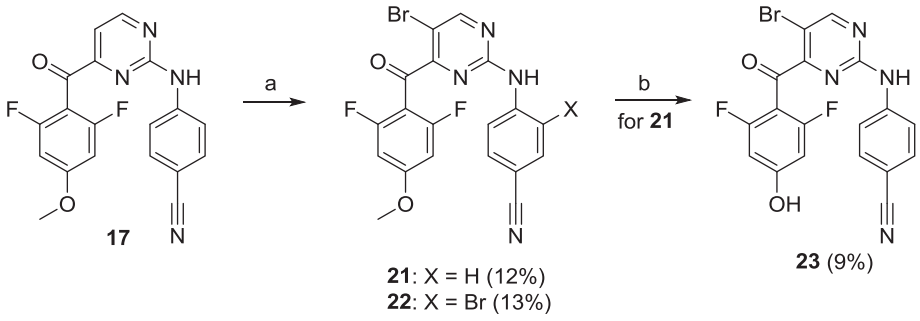

Scheme 4. Reagents and conditions: (a) NBS, DMF, 100 °C, overnight; (b) BBr_3, DCM, r.t., overnight.

limitation. Thus, the most potent compound **17** was also tested towards two major HIV mutant strains K103 N and Y181C (Table 2). Regretably, compound **17** did not exhibit any promising activity against the two mutant strains compared to approved antiviral agents etravirine and efavirenz.

2.4. Crystallography results

To investigate the binding mode of the most potent compound **17**, the co-crystal structure with HIV-1 RT was determined. Compound **17** was found to occupy the NNRTI binding pocket akin to previously reported DAPY analogues (Fig. 3) [18]. Near the pyrimidine core, residues E138 from the p51 subunit and K101 from the p66 subunit form a salt bridge which defines part of the pocket. The pyrimidine core is sandwiched between residues L100 and V179 and a hydrogen bond is found between the aniline nitrogen and the carbonyl of K101 (2.7 Å). The pyrimidine nitrogen is also in close proximity to the backbone nitrogen of K101 (3.4 Å) however the distance suggests that it is not forming a strong hydrogen bond. The A arm is relatively coplanar with the pyrimidine core with torsion of 11° out of plane while the B arm is closer to perpendicular with the pyrimidine (torsion 63°). The B arm lies across the aromatic residues Y181 and Y183. The carbonyl linker between the pyrimidine and B arm is well accommodated in the pocket and not forming any specific interactions with the protein.

2.5. Computational modeling

Molecular dockings using Glide XP (Schrodinger 2015) have been performed with various in-house NNRTI X-ray crystal structures to guide compound design. Re-dockings of co-crystal ligands show on the average less than 1 Å RMSD comparing to their crystallographic conformations. Docking modes of compounds **17** and **21** show high overall similarities (Fig. 4). The binding mode change in compound **21**, in comparison to compound **17**, is mainly due to the extra Br group (Fig. 4a). Compound **21** binds in the NNRTI pocket with a less ideal and bigger out-of-plane carbonyl dihedral angel (34°) comparing to compound **17** (24°). The Br—O distance is 3.1 Å which is smaller than sum of individual van der Waals radius ($R_{vdw,Br}$ = 1.9 Å and $R_{vdw,O}$ = 1.6 Å). There is potentially more negative charge repulsion between Br and neighbouring carbonyl group (Fig. 4b). This could explain why compound **21** is less potent than **17** contrary to the potency gains from the Br group in the etravirine series where there is no carbonyl group and the oxygen atom simply acts as the linker between the pyrimidine and phenyl ring.

3. Conclusion

A novel series of NNRTIs was designed that combines structural features of 2,6-difluorophenyl B ring [31] and NNRTI analogues having carbonyl group as a linker between the B aryl ring and central pyrimidine [19]. New synthetic route has been developed to prepare the target NNRTIs, where a reaction of commercially available 2,4-dichloropyrimidine with various arylaldehydes was used as the first step. This approach allowed us to prepare unique

Table 2
Anti-HIV activity of compound **17** against wild type (w.t.) and K103 N and Y181C mutant strains (n = 2).

Compound	EC_{50} (μM) w.t.	EC_{50} (μM) K103 N	EC_{50} (μM) Y181C
17	0.004	0.347	>0.500
Etravirine	0.002	0.002	0.012
Efavirenz	0.001	0.101	0.005

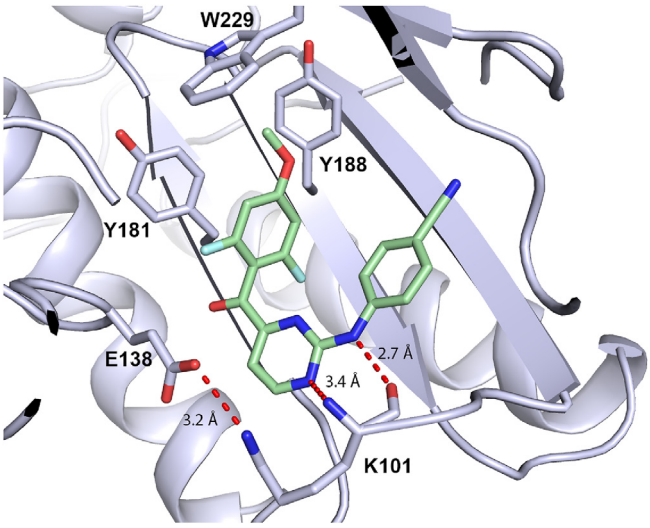

Fig. 3. Co-crystal structure of HIV-1 reverse transcriptase (RT) and compound **17**. Dashed lines show hydrogen bond contacts in the pocket between the compound and the protein.

derivatives with required 2,6-difluorobenzoyl moiety connected to C-4 position of the pyrimidine ring. From the series prepared, compounds **17**–**19** and **21** exhibited nanomolar activities (4–69 nM) against HIV-1 with no significant toxicity. A common feature of these potent compounds is the presence of 2,6-difluorophenyl B arm, that leads to almost perpendicular positioning of B ring with the pyrimidine core. This key conformational feature has been corroborated by determination of co-crystal structure of the most potent compound **17** with HIV-1 RT. On the other hand, compounds **4**–**6** and **9**–**11**, which do not possess this conformational advantage and are practically planar, were shown to be several orders of magnitude less active against HIV-1 compared to their counterparts with both *ortho*-substituents on B phenyl ring. In other words, the conformational rigidity and nearly perpendicular position of the B arm towards pyrimidine core are utterly essential for activity of the reported analogues. Unfortunately, the most potent derivative **17** did not exhibit any interesting antiviral activity against major NNRTI-resistant single mutants K103 N and Y181C. The resistance profile of the reported DAPY series thus needs to be improved within the future antiretroviral drug discovery design. The most potent NNRTIs reported herein, nevertheless, represent a promising starting point in the development of even more efficacious anti-HIV drugs.

4. Experimental part

4.1. Chemistry

Chemical reagents and solvents were of analytical grade and were used as purchased. ^{1}H NMR and ^{13}C NMR spectra were recorded on a Bruker Avance III NMR spectrometer at 600.1 MHz (for ^{1}H) equipped by 5 mm TCI cryoprobehead in DMSO-d_6 (Aldrich, 99.8% D) or CD_3OD (Aldrich, 99.8% D). The chemical shifts are reported in δ units, for standardization the residual peaks of solvents (DMSO-d_6 ^{1}H 2.5 ppm and ^{13}C 39.5 ppm; CD_3OD ^{1}H 3.31 ppm and ^{13}C 49.8 ppm) were used. For details concerning the experimental techniques and methods see part 2.2. Following abbreviations were used to describe peak patterns: Py = corresponds to pyrimidine part of molecule, An = aromatic system bonded to amino (e.g. 4-cyanophenylamino) group, Ar = carbon bonded aromatic system (e.g. 4-cyanobenzoyl). The high resolution mass spectra (HRMS) were measured on LTQ Orbitrap XL spectrometer (Thermofisher

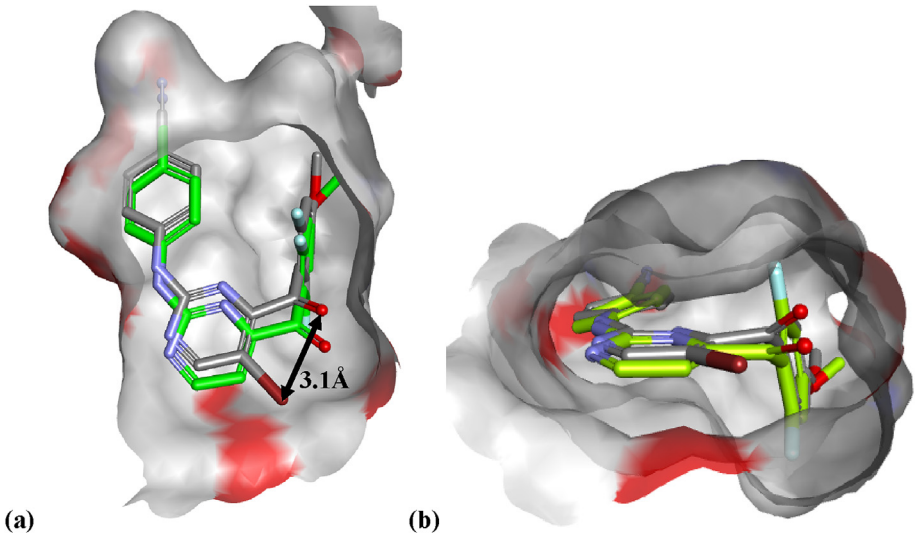

Fig. 4. Docked conformations for compound **17** (green carbon) and **21** (grey carbon) in (a) side view and (b) top view. (For interpretation of the references to colour in this figure legend, the reader is referred to the web version of this article.)

Scientific) using ESI ionisation. All the progress of the reactions was monitored by thin-layer chromatography (TLC) on silica gel plates at 254 nm under a UV lamp or by Waters UPLC/MS system using water-acetonitrile gradient (0.1% formic acid as modifier) on Phenomenex Gemini-NX 3μ C18 110 Å, 100 × 2.00 mm, flow 0.5 mL/min. Flash chromatography separations were performed on silica gel (300–400 mesh) using Isco Teledyne apparatus. All compounds were standardised before biological testing by preparative HPLC (Waters Delta 600) using water-acetonitrile gradient (0.1% trifluoroacetic acid as modifier) on Phenomenex Gemini 10 μm C18, 250 × 21.2 mm, flow 10 mL/min followed by lyophilisation.

*4.1.1. Preparation of 4-(2-chloropyrimidine-4-carbonyl)benzonitrile (**1**) and 4-(4-chloropyrimidine-2-carbonyl)benzonitrile (**2**)*

Sodium hydride (60% dispersion in mineral oil, 0.5 g, 12 mmol) was added to a solution of 2,4-dichloropyrimidine (1 g, 6.7 mmol), 4-formylbenzonitrile (1 g, 7.6 mmol) and *N*,*N*-dimethylbenzimidazolium iodide (1 g, 3.6 mmol) in anhydrous DMF (100 mL). The reaction mixture was stirred at room temperature for 4 h and poured into ice cold water. The product was extracted with EtOAc (2 × 100 mL). Organic phase was washed with brine (2 × 100 mL), dried over sodium sulphate and evaporated to dryness. Column chromatography on silica gel using gradient from 0% to 50% ethyl acetate in hexane afforded **1** (320 mg, 20%) and **2** (250 mg, 15%).

*4-(2-Chloropyrimidine-4-carbonyl)benzonitrile (**1**).* ^{1}H NMR (600.1 MHz, DMSO-d_6) δ 9.12 (d, J = 4.9 Hz, 1H, Py-H6), 8.15–8.13 (m, 2H, Ar-ortho), 8.08–8.06 (m, 2H, Ar-meta), 8.05 (d, J = 4.9 Hz, 1H, Py-H5); ^{13}C NMR (150.9 MHz, DMSO-d_6) δ 190.11 (C=O), 162.92 (Py-C6), 162.52 (Py-C4), 159.43 (Py-C2), 137.79 (Ar-ipso), 132.44 (Ar-meta), 131.13 (Ar-ortho), 119.46 (Py-C5), 118.06 (CN), 115.73 (Ar-para); HRMS (ESI): Calculated for $C_{12}H_7N_3OCl$ $[M+H]^+$: 244.0278, Found: 244.0271; UPLC/MS (m/z) 243.90 $[M+H]^+$, Tr 3.82 min.

*4-(4-Chloropyrimidine-2-carbonyl)benzonitrile (**2**).* ^{1}H NMR (600.1 MHz, DMSO-d_6) δ 9.02 (d, J = 5.4 Hz, 1H, Py-H6), 8.13–8.11 (m, 2H, Ar-ortho), 8.06–8.04 (m, 2H, Ar-meta), 8.01 (d, J = 5.4 Hz, 1H, Py-H5); ^{13}C NMR (150.9 MHz, DMSO-d_6) δ 188.89 (C=O), 161.04 (Py-C4*), 160.91 (Py-C2*), 159.55 (Py-C6), 138.14 (Ar-ipso), 132.48 (Ar-meta), 131.04 (Ar-ortho), 124.03 (Py-C5), 118.07 (CN), 115.70 (Ar-para); HRMS (ESI): Calculated for $C_{12}H_7N_3OCl$ $[M+H]^+$: 244.0278, Found: 244.0268; UPLC/MS (m/z) 243.71 $[M+H]^+$, Tr 3.63 min.

*4.1.2. (2-Chloropyrimidin-4-yl)(4-methoxyphenyl)methanone (**3**)*

4-Methoxybenzaldehyde (1 mL, 8.2 mmol) and sodium hydride (60% dispersion in mineral oil, 0.5 g, 12 mmol) were added to a solution of 2,4-dichloropyrimidine (1 g, 6.7 mmol) and *N*,*N*-dimethylbenzimidazolium iodide (0.5 g, 1.8 mmol) in anhydrous DMF (50 mL). The reaction mixture was stirred at room temperature for 5 h and poured into ice cold water. The product was extracted with EtOAc (2 × 100 mL). Organic phase was washed with brine (2 × 100 mL), dried over sodium sulphate and evaporated to dryness. Column chromatography on silica gel using gradient from 0% to 50% ethyl acetate in hexane afforded 3 (450 mg, 27%) off-white solid. ^{1}H NMR (600.1 MHz, DMSO-d_6) δ 9.05 (d, J = 4.9 Hz, 1H, Py-H6), 8.00–7.97 (m, 2H, Ar-ortho), 7.93 (d, J = 4.9 Hz, 1H, Py-H5), 7.13–7.10 (m, 2H, Ar-meta), 3.89 (s, 3H, CH_3); ^{13}C NMR (150.9 MHz, DMSO-d_6) δ 189.02 (C=O), 164.80 (Py-C4), 164.21 (Ar-para), 162.45 (Py-C6), 159.36 (Py-C2), 133.19 (Ar-ortho), 126.69 (Ar-ipso), 119.18 (Py-C5), 114.16 (Ar-meta), 55.76 (CH_3); HRMS (ESI): Calculated for $C_{12}H_{10}N_2O_2Cl$ $[M+H]^+$: 249.04253, Found: 249.04262; UPLC/MS (m/z) 248.75 $[M+H]^+$, Tr 3.96 min.

*4.1.3. 4-((4-(4-Cyanobenzoyl)pyrimidin-2-yl)amino)benzonitrile (**4**)*

[22] A solution of **1** (200 mg, 0.82 mmol), 4-aminobenzonitrile (100 mg, 0.85 mmol), palladium(II) acetate (20 mg, 0.09 mmol), 4,5-bis(diphenylphosphino)-9,9-dimethylxanthene (100 mg, 0.17 mmol) and cesium carbonate (1 g, 3.1 mmol) in dry dioxane (5 mL) was heated at 90 °C under argon atmosphere for 3 h. The reaction mixture was evaporated to dryness. Column chromatography on silica gel using gradient from 0% to 100% ethyl acetate in hexane gave **4** (180 mg, 68%). ^{1}H NMR (600.1 MHz, DMSO-d_6) δ 10.47 (bs, 1H, NH), 8.89 (d, J = 4.9 Hz, 1H, Py-H6), 8.17–8.14 (m, 2H, Ar-ortho), 8.08–8.05 (m, 2H, Ar-meta), 7.90–7.87 (m, 2H, An-ortho), 7.70–7.67 (m, 2H, An-meta), 7.43 (d, J = 4.9 Hz, 1H, Py-H5); ^{13}C NMR (150.9 MHz, DMSO-d_6) δ 191.91 (C=O), 160.77 (Py-C6), 160.62 (Py-C4), 158.74 (Py-C2), 144.32 (An-ipso), 138.61 (Ar-ipso), 132.98 (An-meta), 132.41 (Ar-meta), 130.90 (Ar-ortho), 119.41 (An-CN), 118.80 (Py-C5), 118.55 (An-ortho), 118.16 (Ar-CN), 115.47 (Ar-para), 103.03 (An-para); HRMS (ESI): Calculated for $C_{19}H_{11}N_5ONa$ $[M+Na]^+$: 348.08558, Found: 348.08570; UPLC/MS (m/z) 326.12 $[M+H]^+$, Tr 4.13 min.

4.1.4. 4-((2-(4-Cyanobenzoyl)pyrimidin-4-yl)amino)benzonitrile (**5**)

A solution of **2** (200 mg, 0.82 mmol), 4-aminobenzonitrile (100 mg, 0.85 mmol), palladium(II) acetate (20 mg, 0.09 mmol), 4,5-bis(diphenylphosphino)-9,9-dimethylxanthene (100 mg, 0.17 mmol) and cesium carbonate (1 g, 3.1 mmol) in dry dioxane (5 mL) was heated at 90 °C under argon atmosphere for 3 h. The reaction mixture was evaporated to dryness. Column chromatography on silica gel using gradient from 0% to 100% ethyl acetate in hexane gave **5** (140 mg, 53%). ^{1}H NMR (600.1 MHz, DMSO-d_6) δ 10.46 (bs, 1H, NH), 8.55 (d, J = 5.9 Hz, 1H, Py-H6), 8.12–8.09 (m, 2H, Ar-ortho), 8.02–7.99 (m, 2H, Ar-meta), 7.89–7.86 (m, 2H, An-ortho), 7.72–7.69 (m, 2H, An-meta), 7.08 (d, J = 5.9 Hz, 1H, Py-H5); ^{13}C NMR (150.9 MHz, DMSO-d_6) δ 190.26 (C=O), 160.24 (Py-C2), 159.76 (Py-C4), 155.76 (Py-C6), 143.70 (An-ipso), 138.78 (Ar-ipso), 133.14 (An-meta), 132.37 (Ar-meta), 130.78 (Ar-ortho), 119.23 (An-ortho), 119.18 (An-CN), 118.14 (Ar-CN), 115.37 (Ar-ipso), 109.85 (Py-C5), 103.95 (An-para); HRMS (ESI): Calculated for $C_{19}H_{12}N_5O$ $[M+H]^+$: 326.10364, Found: 326.10372; UPLC/MS (m/z) 325.87 $[M+H]^+$, Tr 3.76 min.

4.1.5. 4-((4-(4-Methoxybenzoyl)pyrimidin-2-yl)amino)benzonitrile (**6**) [19].

A solution of **3** (450 mg, 1.81 mmol), 4-aminobenzonitrile (300 mg, 2.54 mmol), palladium(II) acetate (30 mg, 0.13 mmol), 4,5-bis(diphenylphosphino)-9,9-dimethylxanthene (150 mg, 0.26 mmol) and cesium carbonate (2 g, 6.1 mmol) in dry dioxane (10 mL) was heated at 90 °C under argon atmosphere for 1 h. The reaction mixture was evaporated to dryness. Column chromatography on silica gel using gradient from 0% to 100% ethyl acetate in hexane afforded **6** (330 mg, 55%). ^{1}H NMR (600.1 MHz, DMSO-d_6) δ 10.46 (bs, 1H, NH), 8.83 (d, J = 4.8 Hz, 1H, Py-H6), 8.02–7.99 (m, 2H, Ar-ortho), 7.97–7.94 (m, 2H, An-ortho), 7.73–7.70 (m, 2H, An-meta), 7.28 (d, J = 4.8 Hz, 1H, Py-H5), 7.13–7.10 (m, 2H, Ar-meta), 3.88 (s, 3H, CH_3); ^{13}C NMR (150.9 MHz, DMSO-d_6) δ 190.78 (C=O), 163.98 (Ar-para), 163.11 (Py-C4), 160.12 (Py-C6), 158.61 (Py-C2), 144.49 (An-ipso), 133.00 (An-meta), 133.00 (Ar-ortho), 127.24 (Ar-ipso), 119.41 (An-CN), 118.45 (An-ortho), 114.08 (Ar-meta), 111.83 (Py-C5), 102.83 (An-para), 55.71 (CH_3); HRMS (ESI): Calculated for $C_{19}H_{14}N_4O_2Na$ $[M+Na]^+$: 353.10090, Found: 353.10107; UPLC/MS (m/z) 331.03 $[M+H]^+$, Tr 4.22 min.

4.1.6. 4-((4-((4-Cyanophenyl)(hydroxy)methyl)pyrimidin-2-yl)amino)benzonitrile (**7**)

Sodium borohydride (5 mg, 0.13 mmol) was added to a solution of **4** (33 mg, 0.10 mmol) in MeOH (5 mL). The reaction mixture was stirred at room temperature for 1 h and then evaporated to dryness. The product was extracted with EtOAc (10 mL) and washed with water. Organic phase was separated, dried over sodium sulphate and evaporated to dryness to give **7** (14 mg, 43%) as a yellowish powder. ^{1}H NMR (600.1 MHz, CD_3OD) δ 8.49 (d, J = 5.1 Hz, 1H, Py-H6), 7.84–7.81 (m, 2H, An-ortho), 7.73–7.71 (m, 2H, Ar-meta), 7.70–7.68 (m, 2H, Ar-ortho), 7.60–7.57 (m, 2H, An-meta), 7.17 (dd, J = 0.6, 5.1 Hz, 1H, Py-H5), 5.74 (s, 1H, CHO); ^{13}C NMR (150.9 MHz, CD_3OD) δ 174.22 (Py-C4), 160.95 (Py-C2), 160.46 (Py-C6), 150.07 (Ar-ipso), 146.67 (An-ipso), 134.46 (An-meta), 133.80 (Ar-meta), 129.41 (Ar-ortho), 120.91 (An-CN), 120.20 (An-ortho), 120.16 (Ar-CN), 112.97 (Ar-para), 111.16 (Py-C5), 105.18 (An-para), 76.73 (CH); HRMS (ESI): Calculated for $C_{19}H_{13}N_5ONa$ $[M+Na]^+$: 350.10123, Found: 350.10132; UPLC/MS (m/z) 327.88 $[M+H]^+$, Tr 3.75 min.

4.1.7. 4-((2-((4-Cyanophenyl)(hydroxy)methyl)pyrimidin-4-yl)amino)benzonitrile (**8**)

Sodium borohydride (5 mg, 0.13 mmol) was added to a solution of **5** (33 mg, 0.10 mmol) in MeOH (5 mL). The reaction mixture was stirred at room temperature for 1 h and then evaporated to dryness. The product was extracted with EtOAc (10 mL) and washed with water. Organic phase was separated, dried over sodium sulphate and evaporated to dryness to give **8** (25 mg, 76%) as yellowish powder. ^{1}H NMR (600.1 MHz, CD_3OD) δ 8.31 (d, J = 6.8 Hz, 1H, Py-H6), 7.80–7.78 (m, 2H, Ar-meta), 7.76–7.74 (m, 2H, Ar-ortho), 7.75–7.73 (m, 2H, An-ortho), 7.73–7.71 (m, 2H, An-meta), 6.94 (d, J = 6.8 Hz, 1H, Py-H5), 5.96 (s, 1H, CHO); ^{13}C NMR (150.9 MHz, CD_3OD) δ 168.75 (Py-C2), 163.14 (Py-C4), 148.59 (Py-C6), 147.68 (Ar-ipso), 143.57 (An-ipso), 134.78 (An-meta), 134.05 (Ar-meta), 129.66 (Ar-ortho), 123.20 (An-ortho), 120.02 (An-CN), 119.91 (Ar-CN), 113.88 (Ar-para), 109.49 (An-para), 108.62 (Py-C5), 75.26 (CH); HRMS (ESI): Calculated for $C_{19}H_{14}N_5O$ $[M+H]^+$: 328.11929, Found: 328.11945; UPLC/MS (m/z) 327.82 $[M+H]^+$, Tr 3.14 min.

4.1.8. 4-(5-Bromo-2-((4-cyanophenyl)amino)pyrimidine-4-carbonyl)benzonitrile (**9**)

A solution of **4** (410 mg, 1.26 mmol) and *N*-bromosuccinimide (600 mg, 3.37 mmol) in DMF (20 mL) was heated at 100 °C for 5 h and then evaporated to dryness. Column chromatography on silica gel using gradient from 0% to 100% ethyl acetate in hexane afforded **9** (84 mg, 17%) as yellow solid. ^{1}H NMR (600.1 MHz, DMSO-d_6) δ 10.69 (bs, 1H, NH), 8.95 (s, 1H, Py-H6), 8.14–8.11 (m, 2H, Ar-ortho), 8.10–8.07 (m, 2H, Ar-meta), 7.87–7.84 (m, 2H, An-ortho), 7.74–7.71 (m, 2H, An-meta); ^{13}C NMR (150.9 MHz, DMSO-d_6) δ 190.52 (C=O), 161.26 (Py-C6), 161.22 (Py-C4), 157.48 (Py-C2), 143.87 (An-ipso), 136.33 (Ar-ipso), 133.30 (Ar-meta), 133.10 (An-meta), 130.55 (Ar-ortho), 119.28 (An-CN), 118.71 (An-ortho), 117.85 (Ar-CN), 116.92 (Ar-para), 104.70 (Py-C5), 103.45 (An-para); HRMS (ESI): Calculated for $C_{19}H_{10}N_5OBrNa$ $[M+Na]^+$: 425.99609, Found: 425.99615; UPLC/MS (m/z) 404.18 $[M+H]^+$, Tr 4.41 min.

4.1.9. 4-((5-Bromo-4-(4-methoxybenzoyl)pyrimidin-2-yl)amino)benzonitrile (**10**)

A solution of **6** (280 mg, 0.85 mmol) and *N*-bromosuccinimide (400 mg, 2.25 mmol) in DMF (5 mL) was heated at 100 °C overnight and then evaporated to dryness. Column chromatography on silica gel using gradient from 0% to 100% ethyl acetate in hexane afforded **10** (320 mg, 92%) as yellow solid. ^{1}H NMR (600.1 MHz, DMSO-d_6) δ 10.64 (bs, 1H, NH), 8.89 (s, 1H, Py-H6), 7.89–7.86 (m, 4H, Ar-ortho, An-ortho), 7.76–7.73 (m, 2H, An-meta), 7.13–7.10 (m, 2H, Ar-meta), 3.88 (s, 3H, CH_3); ^{13}C NMR (150.9 MHz, DMSO-d_6) δ 189.52 (C=O), 164.66 (Ar-para), 163.21 (Py-C4), 160.63 (Py-C6), 157.32 (Py-C2), 143.99 (An-ipso), 133.09 (An-meta), 132.54 (Ar-ortho), 126.13 (Ar-ipso), 119.31 (An-CN), 118.60 (An-ortho), 114.69 (Ar-meta), 104.69 (Py-C5), 103.27 (An-para), 55.81 (OCH_3); HRMS (ESI): Calculated for $C_{19}H_{13}N_4O_2BrNa$ $[M+Na]^+$: 431.01141, Found: 431.01142; UPLC/MS (m/z) 409.03 $[M+H]^+$, Tr 4.42 min.

4.1.10. Preparation of 4-(5-bromo-4-((4-cyanophenyl)amino)pyrimidine-2-carbonyl)benzonitrile (**11**) and 4-(5-bromo-4-((2-bromo-4-cyanophenyl)amino)pyrimidine-2-carbonyl)benzonitrile (**12**)

A solution of **5** (30 mg, 0.09 mmol) and *N*-bromosuccinimide (120 mg, 0.67 mmol) in DMF (3 mL) was heated at 100 °C for 3 h and then evaporated to dryness. Column chromatography on silica gel using gradient from 0% to 100% ethyl acetate in hexane afforded **11** (1 mg, 3%) as yellow powder and **12** (3 mg, 8%) as yellow solid.

*4-(5-Bromo-4-((4-cyanophenyl)amino)pyrimidine-2-carbonyl)benzonitrile (**11**).* ^{1}H NMR (600.1 MHz, DMSO-d_6) δ 9.55 (bs, 1H, NH), 8.87 (s, 1H, Py-H6), 8.12–8.09 (m, 2H, Ar-ortho), 8.04–8.01 (m, 2H, Ar-meta), 7.91–7.88 (m, 2H, An-ortho), 7.77–7.74 (m, 2H, An-meta); ^{13}C NMR (150.9 MHz, DMSO-d_6) δ 189.79 (C=O), 158.44 (Py-C2), 157.86 (Py-C6), 156.50 (Py-C4), 142.65 (An-ipso), 138.69 (Ar-ipso), 132.62 (An-meta), 132.36 (Ar-meta), 130.77 (Ar-ortho), 122.25 (An-

ortho), 118.93 (An-CN), 118.12 (Ar-CN), 115.37 (Ar-para), 107.49 (Py-C5), 105.70 (An-para); HRMS (ESI): Calculated for $C_{19}H_{10}N_5OBrNa$ $[M+Na]^+$: 425.99609, Found: 425.99614; UPLC/MS (*m*/*z*) 403.99 $[M+H]^+$, Tr 4.07 min.

*4-(5-Bromo-4-((2-bromo-4-cyanophenyl)amino)pyrimidine-2-carbonyl)benzonitrile (**12**).* ^{1}H NMR (600.1 MHz, DMSO-d_6) δ 9.24 (bs, 1H, NH), 8.89 (s, 1H, Py-H6), 8.31 (d, J = 1.9 Hz, 1H, An-H3), 8.06–8.03 (m, 2H, Ar-ortho), 8.02 (d, J = 8.4 Hz, 1H, An-H6), 7.99–7.97 (m, 2H, Ar-meta), 7.88 (dd, J = 1.9, 8.4 Hz, 1H, An-H5); ^{13}C NMR (150.9 MHz, DMSO-d_6) δ 189.43 (C=O), 158.55 (Py-C2), 157.52 (Py-C6), 156.71 (Py-C4), 140.94 (An-C1), 138.42 (Ar-ipso), 136.31 (An-C3), 132.29 (Ar-meta), 132.29 (An-C5), 130.74 (Ar-ortho), 126.86 (An-C6), 119.35 (An-C4), 118.05 (Ar-CN), 117.27 (An-CN), 115.38 (Ar-para), 109.31 (An-C2), 107.15 (Py-C5); HRMS (ESI): Calculated for $C_{19}H_9N_5OBr_2Na$ $[M+Na]^+$: 503.90661, Found: 503.90675; UPLC/MS (*m*/*z*) 482.05 $[M+H]^+$, Tr 4.52 min.

4.1.11. (2-Chloropyrimidin-4-yl)(2,6-difluoro-4-methoxyphenyl) methanone (**13**)

Method A: Sodium hydride (60% dispersion in mineral oil, 1.2 g, 29 mmol) was added to a solution of 2,4-dichloropyrimidine (3 g, 20 mmol), 2,6-difluoro-4-methoxybenzaldehyde (4 g, 23 mmol) and *N*,*N*-dimethylbenzimidazolium iodide (1 g, 3.6 mmol) in anhydrous dioxane (50 mL). The reaction mixture was heated under argon at 90 °C for 14 h and poured into ice cold water. The product was extracted with EtOAc (2 × 100 mL). Organic phase was washed with brine (2 × 100 mL), dried over sodium sulphate and evaporated to dryness. Column chromatography on silica gel using gradient from 0% to 50% ethyl acetate in hexane afforded **13** (4.15 g, 73%) as yellowish powder. ^{1}H NMR (600.1 MHz, DMSO-d_6) δ 8.43 (d, J = 4.9 Hz, 1H, Py-H6), 7.33 (d, J = 4.9 Hz, 1H, Py-H5), 6.24 (dd, J = 1.6, 12.1 Hz, 2H, Ar-meta), 3.19 (s, 3H, CH_3); ^{13}C NMR (150.9 MHz, DMSO-d_6) δ 186.06 (CO), 164.59 (t, J = 15.0 Hz, Ar-para), 163.36 (Py-C6), 162.52 (Py-C4), 161.68 (dd, J = 10.0, 252.4 Hz, Ar-ortho), 160.02 (Py-C2), 117.70 (Py-C5), 106.64 (t, J = 17.9 Hz, Ar-ipso), 99.10 (dd, J = 3.5, 28.4 Hz, Ar-meta), 56.72 (OCH_3); HRMS (ESI): Calculated for $C_{12}H_8N_2O_2ClF_2$ $[M+H]^+$: 285.02369, Found: 285.02372; UPLC/MS (*m*/*z*) 284.85 $[M+H]^+$, Tr 4.10 min.

4.1.12. (2-Chloropyrimidin-4-yl)(2,4,6-trifluorophenyl)methanone (**14**)

Treatment of 2,4-dichloropyrimidine (0.75 g, 5 mmol), 2,4,6-trifluorobenzaldehyde (1 g, 6.2 mmol), *N*,*N*-dimethylbenzimidazolium iodide (0.25 g, 0.9 mmol), and sodium hydride (60% dispersion in mineral oil, 0.3 g, 7 mmol) in anhydrous dioxane (10 mL) by Method A afforded **14** (840 mg, 62%) as yellowish powder. ^{1}H NMR (600.1 MHz, DMSO-d_6) δ 9.03 (d, J = 4.9 Hz, 1H, Py-H6), 8.03 (d, J = 4.9 Hz, 1H, Py-H5), 7.48–7.43 (m, 2H, Ar-meta); ^{13}C NMR (150.9 MHz, DMSO-d_6) δ 186.14 (CO), 164.57 (dt, J = 16.1, 243.5 Hz, Ar-para), 163.71 (Py-C6), 161.01 (Py-C4), 160.78 (ddd, J = 9.7, 16.1, 254.0 Hz, Ar-ortho), 160.23 (Py-C2), 117.79 (Py-C5), 111.10 (dt, J = 4.5, 19.0 Hz, Ar-ipso), 101.90 (dt, J = 3.3, 26.9 Hz, Ar-meta); HRMS (ESI): Calculated for $C_{11}H_5N_2OClF_3$ $[M+H]^+$: 273.00370, Found: 273.00363; UPLC/MS (*m*/*z*) 272.88 $[M+H]^+$, Tr 4.13 min.

4.1.13. (2-Chloropyrimidin-4-yl)(4-bromo-2,6-difluorophenyl) methanone (**15**)

Treatment of 2,4-dichloropyrimidine (3 g, 20 mmol), 4-bromo-2,6-difluorobenzaldehyde (4 g, 18 mmol), *N*,*N*-dimethylbenzimidazolium iodide (1 g, 3.6 mmol), and sodium hydride (60% dispersion in mineral oil, 1.2 g, 29 mmol) by Method A gave **15** (1.9 g, 28%) as yellowish solid. ^{1}H NMR (600.1 MHz, DMSO-d_6) δ 9.18 (d, J = 4.9 Hz, 1H, Py-H6), 8.12 (d, J = 4.9 Hz, 1H, Py-H5), 7.77–7.75 (m, 2H, Ar-meta); ^{13}C NMR (150.9 MHz, DMSO-d_6) δ 186.35 (CO), 163.75 (Py-C6), 161.91 (Py-C4), 160.69 (Py-C2), 160.26 (dd, J = 8.0, 256.6 Hz, Ar-ortho), 126.34 (t, J = 12.7 Hz, Ar-para), 117.73 (Py-C5), 116.47 (dd, J = 4.4, 24.1 Hz, Ar-meta), 113.49 (t, J = 19.1 Hz, Ar-ipso); HRMS (ESI): Calculated for $C_{11}H_4N_2OBrClF_2Na$ $[M+Na]^+$: 354.90558, Found: 354.90567; UPLC/MS (*m*/*z*) 332.99 $[M+H]^+$, Tr 4.49 min.

4.1.14. 4-(2-Chloropyrimidine-4-carbonyl)-3,5-difluorobenzonitrile (**16**)

A solution of **15** (1300 mg, 3.9 mmol), zinc(II) cyanide (800 mg, 6.8 mmol) and bis(tri-*t*-butylphosphine)palladium(0) (300 g, 0.59 mmol) in DMF (15 mL) was heated under argon at 80 °C for 1 h. The reaction mixture was evaporated to dryness and column chromatography on silica gel using gradient from 0% to 10% methanol in chloroform afforded **16** (960 mg, 88%) as yellowish powder. ^{1}H NMR (600.1 MHz, DMSO-d_6) δ 9.20 (d, J = 4.9 Hz, 1H, Py-H6), 8.18 (d, J = 4.9 Hz, 1H, Py-H5), 8.08–8.05 (m, 2H, Ar-meta); ^{13}C NMR (150.9 MHz, DMSO-d_6) δ 186.09 (CO), 163.94 (Py-C6), 160.32 (Py-C4), 159.83 (Py-C2), 159.30 (dd, J = 7.7, 254.3 Hz, Ar-ortho), 118.72 (t, J = 20.0 Hz, Ar-ipso), 117.73 (Py-C5), 117.20 (dd, J = 4.5, 24.0 Hz, Ar-meta), 116.34 (t, J = 12.7 Hz, Ar-para), 116.07 (t, J = 3.3 Hz, CN); HRMS (ESI): Calculated for $C_{12}H_5N_3OClF_2$ $[M+H]^+$: 280.00837, Found: 280.00847; UPLC/MS (*m*/*z*) 280.06 $[M+H]^+$, Tr 4.00 min.

4.1.15. 4-((4-(2,6-Difluoro-4-methoxybenzoyl)pyrimidin-2-yl) amino)benzonitrile (**17**)

A solution of **13** (1000 mg, 3.51 mmol), 4-aminobenzonitrile (500 mg, 4.24 mmol), palladium(II) acetate (100 mg, 0.45 mmol), 4,5-bis(diphenylphosphino)-9,9-dimethylxanthene (500 mg, 0.85 mmol), and cesium carbonate (5 g, 15.5 mmol) in dry dioxane (10 mL) was heated at 90 °C under argon atmosphere for 3 h. The reaction mixture was evaporated to dryness. Column chromatography on silica gel using gradient from 0% to 100% ethyl acetate in hexane gave **17** (780 mg, 60%) as yellowish solid. ^{1}H NMR (600.1 MHz, DMSO-d_6) δ 10.48 (bs, 1H, NH), 8.90 (d, J = 4.9 Hz, 1H, Py-H6), 7.82–7.79 (m, 2H, An-ortho), 7.63–7.60 (m, 2H, An-meta), 7.45 (d, J = 4.9 Hz, 1H, Py-H5), 6.98 (dd, J = 1.3, 11.6 Hz, 2H, Ar-meta), 3.91 (s, 3H, CH_3); ^{13}C NMR (150.9 MHz, DMSO-d_6) δ 188.30 (CO), 163.90 (t, J = 14.7 Hz, Ar-para), 161.19 (dd, J = 10.5, 250.2 Hz, Ar-ortho), 161.18 (Py-C6), 160.25 (Py-C4), 159.32 (Py-C2), 144.25 (An-ipso), 132.80 (An-meta), 119.31 (An-CN), 118.44 (An-ortho), 109.98 (Py-C5), 107.72 (t, J = 19.5 Hz, Ar-ipso), 103.03 (An-para), 99.00 (dd, J = 3.2, 25.1 Hz, Ar-meta), 56.71 (OCH_3); HRMS (ESI): Calculated for $C_{19}H_{13}N_4O_2F_2$ $[M+H]^+$: 367.10011, Found: 367.10012; UPLC/MS (*m*/*z*) 367.07 $[M+H]^+$, Tr 4.32 min.

4.1.16. 4-((4-(2,4,6-Trifluorobenzoyl)pyrimidin-2-yl)amino) benzonitrile (**18**)

A solution of **14** (273 mg, 1.0 mmol), 4-aminobenzonitrile (200 mg, 1.7 mmol), palladium(II) acetate (20 mg, 0.09 mmol), 4,5-bis(diphenylphosphino)-9,9-dimethylxanthene (100 mg, 0.17 mmol), and cesium carbonate (1 g, 3.1 mmol) in dry dioxane (5 mL) was heated at 100 °C under argon atmosphere for 1 h. The reaction mixture was evaporated to dryness. Flash column chromatography on silica gel using gradient from 0% to 10% methanol in chloroform afforded **18** (80 mg, 23%) as yellowish solid. ^{1}H NMR (600.1 MHz, DMSO-d_6) δ 10.47 (bs, 1H, NH), 8.94 (d, J = 4.8 Hz, 1H, Py-H6), 7.76–7.73 (m, 2H, An-ortho), 7.63–7.60 (m, 2H, An-meta), 7.52 (d, J = 4.8 Hz, 1H, Py-H5), 7.49–7.46 (m, 2H, Ar-meta); ^{13}C NMR (150.9 MHz, DMSO-d_6) δ 188.21 (CO), 163.98 (dt, J = 15.9, 252.2 Hz, Ar-para), 161.53 (Py-C6), 160.13 (ddd, J = 10.3, 15.8, 251.5 Hz, Ar-ortho), 159.43 (Py-C4), 158.78 (Py-C2), 144.05 (An-ipso), 132.69 (An-meta), 119.17 (An-CN), 118.43 (An-ortho), 112.25 (dt, J = 4.3, 20.5 Hz, Ar-ipso), 109.86 (Py-C5), 103.19 (An-para),

101.60 (dt, J = 2.9, 26.9 Hz, Ar-para); HRMS (ESI): Calculated for $C_{18}H_9N_4OF_3Na$ $[M+Na]^+$: 377.06207, Found: 377.06213; UPLC/MS (m/z) 354.97 $[M+H]^+$, Tr 4.35 min.

4.1.17. 4-(2-((4-Cyanophenyl)amino)pyrimidine-4-carbonyl)-3,5-difluorobenzonitrile (**19**)

A solution of **16** (200 mg, 0.72 mmol), 4-aminobenzonitrile (150 mg, 1.27 mmol), palladium(II) acetate (25 mg, 0.11 mmol), 4,5-bis(diphenylphosphino)-9,9-dimethylxanthene (120 mg, 0.21 mmol), and cesium carbonate (1.2 g, 3.68 mmol) in dry dioxane (5 mL) was heated at 80 °C under argon atmosphere for 1 h. The reaction mixture was diluted with EtOAc (20 mL) and washed with brine (20 mL). Solvent was evaporated and column chromatography on silica gel using gradient from 0% to 10% methanol in chloroform gave **19** (80 mg, 31%) as yellowish solid. ^{1}H NMR (600.1 MHz, DMSO-d_6) δ 10.49 (bs, 1H, NH), 8.97 (d, J = 4.8 Hz, 1H, Py-H6), 8.11–8.07 (m, 2H, Ar-meta), 7.68–7.65 (m, 2H, An-ortho), 7.62–7.59 (m, 2H, An-meta), 7.57 (d, J = 4.8 Hz, 1H, Py-H5); ^{13}C NMR (150.9 MHz, DMSO-d_6) δ 188.00 (CO), 161.77 (Py-C6), 159.44 (Py-C4), 158.80 (dd, J = 18.4, 252.1 Hz, Ar-ortho), 157.66 (Py-C2), 143.85 (An-ipso), 132.62 (An-meta), 120.31 (t, J = 21.5 Hz, Ar-ipso), 119.07 (An-CN), 118.38 (An-ortho), 116.97 (dd, J = 15.5, 23.4 Hz, Ar-meta), 116.04 (t, J = 2.8 Hz, Ar-CN), 115.44 (t, J = 12.5 Hz, Ar-para), 109.68 (Py-C5), 103.29 (An-para); HRMS (ESI): Calculated for $C_{19}H_9N_5OF_2Na$ $[M+Na]^+$: 384.06674, Found: 384.06685; UPLC/MS (m/z) 362.09 $[M+H]^+$, Tr 4.26 min.

4.1.18. 4-((4-(4-((4-Cyanophenyl)amino)-2,6-difluorobenzoyl)pyrimidin-2-yl)amino)benzonitrile (**20**)

A solution of **15** (100 mg, 0.30 mmol), 4-aminobenzonitrile (50 mg, 0.42 mmol), palladium(II) acetate (10 mg, 0.04 mmol), 4,5-bis(diphenylphosphino)-9,9-dimethylxanthene (50 mg, 0.09 mmol), and cesium carbonate (0.5 g, 1.53 mmol) in dry dioxane (3 mL) was heated at 80 °C under argon atmosphere for 1 h. The reaction mixture was evaporated to dryness and column chromatography on silica gel using gradient from 0% to 100% ethyl acetate in hexane gave **20** (25 mg, 18%) as yellowish solid. ^{1}H NMR (600.1 MHz, DMSO-d_6) δ 10.49 (bs, 1H, NH), 9.76 (bs, 1H, NH), 8.89 (d, J = 4.9 Hz, 1H, Py-H6), 7.87–7.84 (m, 2H, An-ortho), 7.79–7.76 (m, 2H, ArAn-meta), 7.65–7.62 (m, 2H, An-meta), 7.41 (d, J = 4.9 Hz, 1H, Py-H5), 7.38–7.35 (m, 2H, ArAn-ortho), 6.96–6.91 (m, 2H, Ar-meta); ^{13}C NMR (150.9 MHz, DMSO-d_6) δ 187.76 (CO), 161.60 (dd, J = 10.2, 250.6 Hz, Ar-ortho), 161.04 (Py-C6), 160.90 (Py-C4), 159.24 (Py-C2), 147.48 (t, J = 14.2 Hz, Ar-para), 144.91 (AnAr-ipso), 144.32 (An-ipso), 133.89 (ArAn-meta), 132.83 (An-meta), 119.32 (An-CN), 119.19 (ArAn-CN), 118.44 (An-ortho), 118.30 (ArAn-ortho), 110.01 (Py-C5), 106.93 (t, J = 19.0 Hz, Ar-ipso), 103.31 (ArAn-para), 102.97 (An-para), 99.69 (dd, J = 3.6, 24.5 Hz, Ar-meta); HRMS (ESI): Calculated for $C_{25}H_{14}N_6OF_2Na$ $[M+Na]^+$: 475.10894, Found: 475.10896; UPLC/MS (m/z) 453.32 $[M+H]^+$, Tr 4.38 min.

4.1.19. Preparation of 4-((5-bromo-4-(2,6-difluoro-4-methoxybenzoyl)pyrimidin-2-yl)amino)benzonitrile (**21**) and 3-bromo-4-((5-bromo-4-(2,6-difluoro-4-methoxybenzoyl)pyrimidin-2-yl)amino)benzonitrile (**22**)

A solution of **17** (100 mg, 0.27 mmol) and *N*-bromosuccinimide (100 mg, 0.56 mmol) in DMF (3 mL) was heated at 90 °C for 1 h and evaporated to dryness. Column chromatography on silica gel using gradient from 0% to 100% ethyl acetate in hexane gave **21** (14 mg, 12%) as yellow solid and **22** (18 mg, 13%) as yellow solid.

*4-((5-Bromo-4-(2,6-difluoro-4-methoxybenzoyl)pyrimidin-2-yl)amino)benzonitrile (**21**).* ^{1}H NMR (600.1 MHz, DMSO-d_6) δ 10.62 (bs, 1H, NH), 8.94 (s, 1H, Py-H6), 7.83–7.80 (m, 2H, An-ortho), 7.71–7.68 (m, 2H, An-meta), 6.97 (dd, J = 1.6, 12.6 Hz, 2H, Ar-meta), 3.57 (s, 3H, OCH_3); ^{13}C NMR (150.9 MHz, DMSO-d_6) δ 184.77 (CO), 165.57 (t, J = 14.8 Hz, Ar-para), 162.52 (dd, J = 10.1, 256.1 Hz, Ar-ortho), 161.64 (Py-C4), 161.64 (Py-C6), 157.55 (Py-C2), 143.84 (An-ipso), 133.05 (An-meta), 119.28 (An-CN), 118.68 (An-ortho), 106.71 (t, J = 14.6 Hz, Ar-ipso), 103.71 (Py-C5), 103.49 (An-para), 99.50 (dd, J = 3.6, 27.1 Hz, Ar-meta), 56.97 (OCH_3); HRMS (ESI): Calculated for $C_{19}H_{12}N_4O_2BrF_2$ $[M+H]^+$: 445.01062, Found: 445.01062; UPLC/MS (m/z) 445.19 $[M+H]^+$, Tr 4.52 min.

*3-Bromo-4-((5-bromo-4-(2,6-difluoro-4-methoxybenzoyl)pyrimidin-2-yl)amino)benzonitrile (**22**).* ^{1}H NMR (600.1 MHz, DMSO-d_6) δ 9.66 (bs, 1H, NH), 8.83 (s, 1H, Py-H6), 8.17 (dd, J = 0.4, 1.8 Hz, 1H, An-H3), 7.82 (dd, J = 0.4, 8.5 Hz, 1H, An-H6), 7.78 (dd, J = 1.8, 8.5 Hz, 1H, An-H5), 6.94 (dd, J = 1.5, 12.6 Hz, 2H, Ar-meta), 3.90 (s, 3H, OCH_3); ^{13}C NMR (150.9 MHz, DMSO-d_6) δ 184.82 (CO), 165.56 (t, J = 15.5 Hz, Ar-para), 162.53 (dd, J = 9.5, 255.9 Hz, Ar-ortho), 161.96 (Py-C4), 161.63 (Py-C6), 158.07 (Py-C2), 141.75 (An-C1), 136.47 (An-C3), 132.04 (An-C5), 125.71 (An-C6), 118.02 (An-C2), 117.52 (An-CN), 108.09 (An-C4), 106.59 (t, J = 15.0 Hz, Ar-ipso), 103.70 (Py-C5), 99.56 (dd, J = 4.2, 27.1 Hz, Ar-meta), 56.96 (OCH_3); HRMS (ESI): Calculated for $C_{19}H_{11}N_4O_2Br_2F_2$ $[M+H]^+$: 522.92113, Found: 522.92096; UPLC/MS (m/z) 523.13 $[M+H]^+$, Tr 4.87 min.

4.1.20. 4-((5-Bromo-4-(2,6-difluoro-4-hydroxybenzoyl)pyrimidin-2-yl)amino)benzonitrile (**23**)

A solution of boron tribromide (1.5 mL, 1 M in methylene chloride, 1.5 mmol) was added to a solution of **21** (125 mg, 0.28 mmol) in methylene chloride (4 mL) at 0 °C. The reaction mixture was stirred overnight at room temperature. MeOH (3 mL) was added dropwise and the reaction mixture was evaporated to dryness. Column chromatography on silica gel using gradient from 0% to 10% methanol in chloroform gave **23** (11 mg, 9%) as of-white solid. ^{1}H NMR (600.1 MHz, DMSO-d_6) δ 10.62 (bs, 1H, NH), 8.91 (s, 1H, Py-H6), 7.85–7.81 (m, 2H, An-ortho), 7.73–7.69 (m, 2H, An-meta), 6.61 (dd, J = 1.4, 12.6 Hz 2H, Ar-meta); ^{13}C NMR (150.9 MHz, DMSO-d_6) δ 183.91 (CO), 165.80 (t, J = 14.7 Hz, Ar-para), 163.42 (dd, J = 19.7, 255.8 Hz, Ar-ortho), 162.90 (Py-C4), 161.79 (Py-C6), 158.05 (Py-C2), 144.37 (An-ipso), 133.48 (An-meta), 119.73 (An-CN), 119.18 (An-ortho), 105.63 (t, J = 15.5 Hz, Ar-ipso), 104.13 (Py-C5), 103.97 (An-para), 100.81 (dd, J = 3.7, 24.9 Hz, Ar-meta); HRMS (ESI): Calculated for $C_{18}H_9N_4O_2BrF_2Na$ $[M+Na]^+$: 452.97692, Found: 452.97691; UPLC/MS (m/z) 431.08 $[M+H]^+$, Tr 4.17 min.

4.2. MT-4 HIV antiviral and cytotoxicity assay

Compounds were tested in a high-throughput 384-well assay format for their ability to inhibit the replication of HIV-1 (IIIB) in MT-4 cells. Compounds were serially diluted (1:3) in DMSO on 384-well polypropylene plates and further diluted 200-fold into complete RPMI media (10% FBS, 1% P/S) using the Biotek Micro Flow and Agilent ECHO acoustic dispenser. Each plate contained up to 8 test compounds, with negative (No Drug Control) and 5 μM AZT positive controls. MT-4 cells were pre-infected with 10 μL of either RPMI (mock-infected) or a fresh 1:250 dilution of an HIV-1 (IIIB) concentrated virus stock. Infected and uninfected MT-4 cells were further diluted in complete RPMI media and added to each plate using a Micro Flow dispenser. After 5 days incubation in a humidified and temperature controlled incubator (37 °C), Cell Titer Glo (Promega) was added to the assay plates to quantify the amount of luciferase. EC_{50} and CC_{50} values were defined as the compound concentration that causes a 50% decrease in luminescence signal, and were calculated using a sigmoidal dose-response model to generate curve fits.

4.3. RT co-crystallization, data collection, and structure refinement

Co-crystals of the HIV-1 RT and **17** were grown by hanging drop

Table 3
X-ray data collection and refinement statistics for compound **17**.

Data collection	
Space group	$C222_1$
Resolution (Å)	50.00–2.40 (2.45–2.40)
No. unique	53 535
I/σ	28.7 (2.4)
R_{merge}[a] (%)	5.8 (70.1)
Completeness (%)	96.6 (98.2)
Refinement statistics	
Resolution (Å)	50.0–2.4
No. reflections ($F \geq 0$)	51 444
R-factor[b]	20,4
R-free[b]	26,3
RMS bond lengths (Å)	0,009
RMS bond angles (°)	1,19

[a] $Rmerge = [\sum h \sum i |Ih - Ihi| / \sum h \sum i Ihi]$ where Ih is the mean of Ihi observations of reflection h. Numbers in parenthesis represent highest resolution shell.

[b] *R*-factor and *R*-free $= \sum ||Fobs| - |Fcalc|| / \sum |Fobs| \times 100$ for 95% of recorded data (*R*-factor) or 5% of data (*R*-free).

vapor diffusion as described previously [18]. Briefly, purified RT was concentrated and combined with **17** to a final concentration of 20 mg/ml RT and 0.5 mM **17**. This protein/inhibitor solution was mixed in equal parts with mother liquor containing 0.8 M K/Na tartrate and MES pH 6.5 at 20 °C. Prior to data collection, the crystals were transferred into a solution of 25% glycerol in addition to the mother liquor and then cryocooled in liquid nitrogen. Data was collected at a temperature of 100 K and processed with HKL2000 [35].

Molecular replacement and structure refinement was performed with Phenix [36] using the starting model PDB code 3MEE. Model building was performed with the molecular graphics program Coot [37]. The final model statistics are listed in Table 3 and the data have been deposited into the Protein Data Bank (PDB code: 5K14).

Acknowledgements

This work was supported by the subvention for development of research organization (Institute of Organic Chemistry and Biochemistry CAS, RVO 61388963).

Appendix A. Supplementary data

Supplementary data related to this article can be found at http://dx.doi.org/10.1016/j.ejmech.2016.06.026.

References

[1] J.V. Madruga, P. Cahn, B. Grinsztejn, R. Haubrich, J. Lalezari, A. Mills, G. Pialoux, T. Wilkin, M. Peeters, J. Vingerhoets, G. de Smedt, L. Leopold, R. Trefiglio, B. Woodfall, Efficacy and safety of TMC125 (etravirine) in treatment-experienced HIV-1-infected patients in DUET-1: 24-week results from a randomised, double-blind, placebo-controlled trial, Lancet 370 (2007) 29–38.
[2] A. Lazzarin, T. Campbell, B. Clotet, M. Johnson, C. Katlama, A. Moll, W. Towner, B. Trottier, M. Peeters, J. Vingerhoets, G. de Smedt, B. Baeten, G. Beets, R. Sinha, B. Woodfall, Efficacy and safety of TMC125 (etravirine) in treatment-experienced HIV-1-infected patients in DUET-2: 24-week results from a randomised, double-blind, placebo-controlled trial, Lancet 370 (2007) 39–48.
[3] A.M. Geretti, Shifting paradigms: the resistance profile of etravirine, J. Antimicrob. Chemother. 62 (2008) 643–647.
[4] P.A. Janssen, P.J. Lewi, E. Arnold, F. Daeyaert, M. De Jonge, J. Heeres, L. Koymans, M. Vinkers, J. Guillemont, E. Pasquier, M. Kukla, D. Ludovici, K. Andries, M.P. de Bethune, R. Pauwels, K. Das, A.D. Clark Jr., Y.V. Frenkel, S.H. Hughes, B. Medaer, F. De Knaep, H. Bohets, F. De Clerck, A. Lampo, P. Williams, P. Stoffels, In search of a novel anti-HIV drug: multidisciplinary coordination in the discovery of 4-[[4-[[4-[(1E)-2-cyanoethenyl]-2,6-dimethylphenyl]amino]-2-pyrimidinyl]amino]benzonitrile (R278474, rilpivirine), J. Med. Chem. 48 (2005) 1901–1909.
[5] L. Baert, G. van't Klooster, W. Dries, M. Francois, A. Wouters, E. Basstanie, K. Iterbeke, F. Stappers, P. Stevens, L. Schueller, P. Van Remoortere, G. Kraus, P. Wigerinck, J. Rosier, Development of a long-acting injectable formulation with nanoparticles of rilpivirine (TMC278) for HIV treatment, Eur. J. Pharm. Biopharm. 72 (2009) 502–508.
[6] M.-P. de Bethune, Non-nucleoside reverse transcriptase inhibitors (NNRTIs), their discovery, development, and use in the treatment of HIV-1 infection: a review of the last 20 years (1989–2009), Antivir. Res. 85 (2010) 75–90.
[7] C. Reynolds, C.B. de Koning, S.C. Pelly, W.A. van Otterlo, M.L. Bode, In search of a treatment for HIV – current therapies and the role of non-nucleoside reverse transcriptase inhibitors (NNRTIs), Chem. Soc. Rev. 41 (2012) 4657–4670.
[8] E. De Clercq, The role of non-nucleoside reverse transcriptase inhibitors (NNRTIs) in the therapy of HIV-1 infection, Antivir. Res. 38 (1998) 153–179.
[9] P. Zhan, X. Chen, D. Li, Z. Fang, E. De Clercq, X. Liu, HIV-1 NNRTIs: structural diversity, pharmacophore similarity, and implications for drug design, Med. Res. Rev. 33 (2013) E1–E72.
[10] E. De Clercq, Non-nucleoside reverse transcriptase inhibitors (NNRTIs): past, present, and future, Chem. Biodivers. 1 (2004) 44–64.
[11] X. Chen, P. Zhan, D. Li, E. De Clercq, X. Liu, Recent advances in DAPYs and related analogues as HIV-1 NNRTIs, Curr. Med. Chem. 18 (2011) 359–376.
[12] P. Zhan, X. Liu, Z. Li, Recent advances in the discovery and development of novel HIV-1 NNRTI platforms: 2006-2008 update, Curr. Med. Chem. 16 (2009) 2876–2889.
[13] P. Zhan, X. Liu, Novel HIV-1 non-nucleoside reverse transcriptase inhibitors: a patent review (2005-2010), Expert Opin. Ther. Pat. 21 (2011) 717–796.
[14] D. Li, P. Zhan, E. De Clercq, X. Liu, Strategies for the design of HIV-1 non-nucleoside reverse transcriptase inhibitors: lessons from the development of seven representative paradigms, J. Med. Chem. 55 (2012) 3595–3613.
[15] X. Li, L. Zhang, Y. Tian, Y. Song, P. Zhan, X. Liu, Novel HIV-1 non-nucleoside reverse transcriptase inhibitors: a patent review (2011-2014), Expert Opin. Ther. Pat. 24 (2014) 1199–1227.
[16] Y. Song, Z. Fang, P. Zhan, X. Liu, Recent advances in the discovery and development of novel HIV-1 NNRTI platforms (Part II): 2009-2013 update, Curr. Med. Chem. 21 (2014) 329–355.
[17] P. Zhan, C. Pannecouque, E. De Clercq, X. Liu, Anti-HIV drug discovery and development: current innovations and future trends, J. Med. Chem. 59 (2016) 2849–2878.
[18] E.B. Lansdon, K.M. Brendza, M. Hung, R. Wang, S. Mukund, D. Jin, G. Birkus, N. Kutty, X. Liu, Crystal structures of HIV-1 reverse transcriptase with etravirine (TMC125) and rilpivirine (TMC278): implications for drug design, J. Med. Chem. 53 (2010) 4295–4299.
[19] F.-E. Chen, X.-Q. Feng, Y.-H. Liang, Z.-S. Zeng, CN101723903, 2009.
[20] X.-D. Ma, S.-Q. Yang, S.-X. Gu, Q.-Q. He, F.-E. Chen, E. De Clercq, J. Balzarini, C. Pannecouque, Synthesis and anti-HIV activity of aryl-2-[(4-cyanophenyl) amino]-4-pyrimidinone hydrazones as potent non-nucleoside reverse transcriptase inhibitors, ChemMedChem 6 (2011) 2225–2232.
[21] X.-Q. Feng, Z.-S. Zeng, Y.-H. Liang, F.-E. Chen, C. Pannecouque, J. Balzarini, E. De Clercq, Synthesis and biological evaluation of 4-(hydroxyimino)arylmethyl diarylpyrimidine analogues as potential non-nucleoside reverse transcriptase inhibitors against HIV, Bioorg. Med. Chem. 18 (2010) 2370–2374.
[22] Y. Liu, G. Meng, A. Zheng, F. Chen, W. Chen, E. De Clercq, C. Pannecouque, J. Balzarini, Design and synthesis of a new series of cyclopropylamino-linking diarylpyrimidines as HIV non-nucleoside reverse transcriptase inhibitors, Eur. J. Pharm. Sci. 62 (2014) 334–341.
[23] G. Meng, Y. Liu, A. Zheng, F. Chen, W. Chen, E. De Clercq, C. Pannecouque, J. Balzarini, Design and synthesis of a new series of modified CH-diarylpyrimidines as drug-resistant HIV non-nucleoside reverse transcriptase inhibitors, Eur. J. Med. Chem. 82 (2014) 600–611.
[24] S.-X. Gu, Q.-Q. He, S.-Q. Yang, X.-D. Ma, F.-E. Chen, E. De Clercq, J. Balzarini, C. Pannecouque, Synthesis and structure–activity relationship of novel diarylpyrimidines with hydromethyl linker (CH(OH)-DAPYs) as HIV-1 NNRTIs, Bioorg. Med. Chem. 19 (2011) 5117–5124.
[25] Z.-H. Yan, H.-Q. Wu, W.-X. Chen, Z. Wu, H.-R. Piao, Q.-Q. He, F.-E. Chen, E. De Clercq, C. Pannecouque, Synthesis and biological evaluation of CHX-DAPYs as HIV-1 non-nucleoside reverse transcriptase inhibitors, Bioorg. Med. Chem. 22 (2014) 3220–3226.
[26] Z.-S. Zeng, Y.-H. Liang, X.-Q. Feng, F.-E. Chen, C. Pannecouque, J. Balzarini, E. De Clercq, Lead optimization of diarylpyrimidines as non-nucleoside inhibitors of HIV-1 reverse transcriptase, ChemMedChem 5 (2010) 837–840.
[27] Z.-H. Yan, X.-Y. Huang, H.-Q. Wu, W.-X. Chen, Q.-Q. He, F.-E. Chen, E. De Clercq, C. Pannecouque, Structural modifications of CH(OH)-DAPYs as new HIV-1 non-nucleoside reverse transcriptase inhibitors, Bioorg. Med. Chem. 22 (2014) 2535–2541.
[28] S.-X. Gu, H. Qiao, Y.-Y. Zhu, Q.-C. Shu, H. Liu, X.-L. Ju, E. De Clercq, J. Balzarini, C. Pannecouque, A novel family of diarylpyrimidines (DAPYs) featuring a diatomic linker: design, synthesis and anti-HIV activities, Bioorg. Med. Chem. 23 (2015) 6587–6593.
[29] C. Mordant, B. Schmitt, E. Pasquier, C. Demestre, L. Queguiner, C. Masungi, A. Peeters, L. Smeulders, E. Bettens, K. Hertogs, J. Heeres, P. Lewi, J. Guillemont, Synthesis of novel diarylpyrimidine analogues of TMC278 and their antiviral activity against HIV-1 wild-type and mutant strains, Eur. J. Med. Chem. 42 (2007) 567–579.
[30] D.W. Ludovici, B.L. De Corte, M.J. Kukla, H. Ye, C.Y. Ho, M.A. Lichtenstein, R.W. Kavash, K. Andries, M.-P. de Bethune, H. Azijn, R. Pauwels, P.J. Lewi, J. Heeres, L.M.H. Koymans, M.R. de Jonge, K.J.A. Van Aken, F.F.D. Daeyaert,

K. Das, E. Arnold, P.A.J. Janssen, Evolution of anti-HIV drug candidates. Part 3: diarylpyrimidine (DAPY) analogues, Bioorg. Med. Chem. Lett. 11 (2001) 2235–2239.
[31] D. Rotili, D. Tarantino, M. Artico, M.B. Nawrozkij, E. Gonzalez-Ortega, B. Clotet, A. Samuele, J.A. Esté, G. Maga, A. Mai, Diarylpyrimidine–dihydrobenzyloxopyrimidine hybrids: new, wide-spectrum anti-HIV-1 agents active at (sub)-nanomolar level, J. Med. Chem. 54 (2011) 3091–3096.
[32] S.T. Bedford, K.R. Benwell, T. Brooks, I. Chen, M. Comer, S. Dugdale, T. Haymes, A.M. Jordan, G.A. Kennett, A.R. Knight, B. Klenke, L. LeStrat, A. Merrett, A. Misra, S. Lightowler, A. Padfield, K. Poullennec, M. Reece, H. Simmonite, M. Wong, I.A. Yule, Discovery and optimization of potent and selective functional antagonists of the human adenosine A2B receptor, Bioorg. Med. Chem. Let. 19 (2009) 5945–5949.
[33] A. Miyashita, H. Matsuda, C. Iijima, T. Higashino, Catalytic action of azolim salts. II. Aroylation of 4-chloroquinazolines with aromatic aldehydes catalysed by 1,3-dimethylbenzimidazolium iodide, Chem. Pharm. Bull. 40 (1992) 43–48.
[34] D.S. Surry, S.L. Buchwald, Dialkylbiaryl phosphines in Pd-catalyzed amination: a user's guide, Chem. Sci. 2 (2011) 27–50.
[35] Z.M. Otwinowski, W. Minor, Processing of X-ray diffraction data collection in oscillation mode, in: C.W. Carter Jr., R.M. Sweet (Eds.), Methods in Enzymology 276, Academic Press, New York, 1997, pp. 307–326.
[36] P.D. Adams, P.V. Afonine, G. Bunkoczi, V.B. Chen, I.W. Davis, N. Echols, J.J. Headd, L.-W. Hung, G.J. Kapral, R.W. Grosse-Kunstleve, A.J. McCoy, N.W. Moriarty, R. Oeffner, R.J. Read, D.C. Richardson, J.S. Richardson, T.C. Terwilliger, P.H. Zwart, PHENIX: a comprehensive Python-based system for macromolecular structure solution, Acta Cryst. D66 (2010) 213–221.
[37] P. Emsley, K. Cowtan, Coot: model-building tools for molecular graphics, Acta Cryst. D60 (2004) 2126–2132.